Simulation and patient studies of scatter correction in cardiac SPECT imaging

Mahsa Noori-Asl[1], Ahmad Bitarafan-Rajabi[2,3*]

1. Department of Physics, Faculty of Science, University of Mohaghegh Ardabili, Ardabil, Iran
2. Interventional Research Center, Rajaie Cardiovascular Medical and Research Center, Iran University of Medical Sciences, Tehran, Iran.
3. Echocardiography Research Center, Rajaie Cardiovascular Medical and Research Center, Iran University of Medical Sciences, Tehran, Iran.

ARTICLE INFO	ABSTRACT
	Introduction: Myocardial perfusion imaging is a nuclear medicine imaging method that is used to detect coronary artery diseases. One of the main sources of error in this imaging method is the detection of Compton scattered photons in the photopeak energy window used for data acquisition. This results in the degradation of the image contrast, and therefore decreases the diagnostic accuracy. ***Material and Methods:*** In this study, the efficiency of dual-energy window (DEW) correction method regarding the reduction of the undesirable influence of scattering was investigated using the images acquired from the 3D-NCAT simulated phantom, and a group of patients (18 males and 27 females) in both rest and stressful situations. To evaluate the scatter correction method, the image contrasts are calculated before and after applying the scatter correction. ***Results:*** The results obtained from this study indicated that the calculated image contrasts enhanced by applying the scatter correction in both simulation and patient studies. In the simulation study, the relative values of increase in image contrast are about 10.15% and 12.58% when using a k value equal to 0.5, and the linear fitting method, respectively. In the patient study, the relative values of increase in image contrasts regarding the rest and stress situations were about 13.63% and 10.84% for females and 12.03% and 10.56% for males, respectively. ***Conclusion:*** The utilization of the DEW method for scatter correction of cardiac SPECT images results in an increase in the image contrast and the improvement of the image quality.

Introduction

Myocardial perfusion imaging (MPI) (1) is one of the nuclear medicine imaging methods that is performed by the injection of a radiopharmaceutical into the patient's bloodstream. In this imaging method is usually acquired two sets of images. One set is rest images acquired after an injection at rest situation and another set is stress images obtained after injection during a stressful situation. The stressful situation is usually caused by either exercise on a treadmill or medication called dipyridamole. This imaging is a noninvasive method to detect coronary artery diseases (2).

One of the essential problems in this imaging method is the detection of Compton scattered photons. The detection of the scattered photons results in the degradation of the image contrast, and therefore reduce the quantitative and qualitative accuracy of the images. Therefore, the utilization of a scatter correction method for the elimination or reduction of the scattered photons would be important in diagnosis and treatment. A number of scatter correction methods based on setting additional energy windows in Tc-99m energy spectrum is proposed (3-15) to decrease the contribution of scattered photons in the photopeak energy window.

In a Compton scattering event, the scattered photon moves along a direction different from the direction of the primary incidence photon. Therefore, the detection of Compton scattered photon leads to misleading information about the photon's emission point. Accordingly, the presence of scattered photons in the images obtained from the nuclear medicine imaging systems results in blurring images, and therefore decreases the image contrast.

On the other hand, the energy of these photons is lower than the primary photons. As a result, by limiting the detected photon energies to a given range of the photopeak energy, it is possible to eliminate the scattered photons significantly. Therefore, the first and simplest of the scatter correction method is performed by setting a 20% energy window centered on Tc-99m photopeak energy (140 keV).

Although the utilization of this method leads to a decrease in the scattered photons significantly, but

Corresponding Author: Tel: 09121972366; Email: bitarafan@hotmail.com

some of the scattered photons are still detected in the photopeak energy window. This is due to the limited energy resolution of NaI(Tl) scintillation crystal used in single photon emission computed tomography (SPECT) imaging system (10% FWHM at 140 keV) (14). The second simplest method for the scatter correction is Dual-energy window (DEW) correction method (3, 6, 12, 14). This correction method is performed by setting a secondary energy window in the Compton region on the ⁹⁹ᵐTc energy spectrum. In this study, the 3D-NCAT (Non-uniform rational B-spline-based cardiac-torso) simulated phantom (16) was initially utilized to evaluate the DEW method. In the next step, the images obtained from a group of patients were evaluated to assess the correction method in a realistic situation. The image contrasts obtained before and after applying to scatter correction were compared in both steps.

Materials and Methods

Scatter Correction Method

Dual-energy window (DEW) method which is employed in this study is a simple scatter correction method (3, 13) that can be applied on the nuclear medicine imaging systems. The Tc-99m energy spectrum and energy windows used for this scatter correction method are illustrated in Figure 1. In this correction method, the number of scatter photons (S_{pk}) detected in the photopeak energy window (a 20% energy window centered on Tc-99m photopeak energy [126-154 keV]) are estimated as a factor of the total number of photons (T_C) acquired from an secondary energy window placed in the Compton area of Tc-99m energy spectrum (92-125 keV):

$$S_{pk}(i, j) = kT_C(i, j) \tag{1}$$

Where, (i,j) denotes the pixel's position in the image matrix. Therefore, the corrected photopeak projections (SC_{pk}) will be obtained by subtracting the estimated scatter counts (Eq.1) from the total counts acquired in the photopeak energy window:

$$SC_{pk}(i, j) = T_{pk}(i, j) - S_{pk}(i, j) \tag{2}$$

The scatter correction can be applied before or after the image reconstruction and both of them lead to the same results. In this study, the scatter correction was performed on the projection images. Afterward, the projection images are reconstructed using the filtered back-projection method with Hann filter programmed in MATLAB (Version 7.5.0).
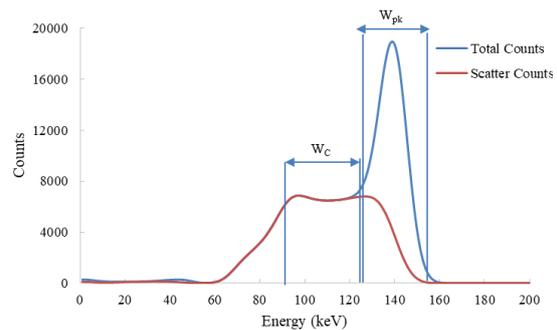

Figure 1. Illustration of the energy windows used in Dual-energy window correction method overlaid on the ⁹⁹ᵐTc energy spectrum. W_{pk} and W_C indicate the photopeak and Compton energy windows, respectively.

Simulation Study

In this study, the SIMIND Monte Carlo simulation program (Version 6.1) (17) was utilized to produce the projection images. One of the advantages of this simulation is its ability to produce the projection images and energy spectra for the scatter and primary counts individually, despite producing them for the total counts. Therefore, the simulation is a suitable instrument to evaluate the scatter correction methods in nuclear medicine imaging.

The SPECT imaging system used for the simulation study includes a cylindrical NaI(Tl) scintillation crystal with a radius of 25 cm and a thickness of 0.95 cm. This system is equipped with a low-energy high-resolution (LEHR) collimator with a thickness of 3.28 cm and the hexagonal holes. The system energy resolution and intrinsic spatial resolution are 10% and 0.34 cm, respectively, at 140 keV.

In order to evaluate the scatter correction method, the simulated 3D-NCAT phantom was employed showing a realistic model of the activity distribution in the normal human body (Fig.2). For different organs of the 3D-NCAT phantom, the activity distributions were utilized that were similar to the distributions used in a study conducted by Segars et al. (Table 1) (18). In total, 32 projection images (64×64 matrices) were obtained by a $180°$ rotation of the gamma camera in a 52 sec elapsed time per projection. The pixel size was set equal to 0.4 cm to investigate the effect of scatter correction on the heart area.
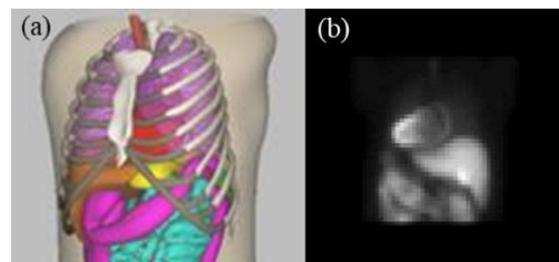

Figure 2. A total view of (a) 3D-NCAT phantom and (b) a projection image of this phantom.

Table 1. The ^{99m}Tc activity concentration used for different organs in the NCAT phantom (18).

Organ	Activity concentration
Heart myocardium, liver, and kidneys	75
Spleen	60
Lungs	4
Stomach, spine, rib, and body	2

In the simulation study, two methods were used to apply the scatter correction as follows:

1) A constant value for the *k* factor: The *k* value proposed by Jaszczak et al. (*k* = 0.5) was utilized in this method (3)

2) A linear fitting method: A graph was initially plotted in this method. The horizontal axis was the pixel counts of an arbitrary projection obtained from the total counts of Compton energy window (T_C (i,j)). In addition, the vertical axis was the pixel counts related to the same projection obtained from the scatter counts of the photopeak energy window (S_{pk} (i,j)).

The linear fitting of these two sets of the data came into the following fitting equation

$$S_{pk}(i, j) = aT_C(i, j) + b \tag{3}$$

Where, *a* and *b* signify the fitting coefficients.

To evaluate the scatter correction method, the image contrasts were calculated using a line profile through the same corrected and uncorrected slices of the reconstructed images of the 3D-NCAT phantom (Fig.3a). The image contrast (*C*) obtained from this profile is defined as follows (14):

$$C = \frac{Mean_{two\ peaks} - V}{Mean_{two\ peaks}} \tag{4}$$

Figure 3b illustrates the two peaks and a valley for an arbitrary profile.

Patient study

A group of patients, including 27 females and 18 males were investigated to evaluate the effect of the scatter correction method on a realistic clinical situation. In total, 32 projections (64×64 matrices) were acquired by a 180° rotation of the gamma camera around the patients with the step-and-shoot mode in a 30 sec elapsed time per projection. All images were acquired by SIEMENS SPECT imaging system.

In the first step, the patient history forms were studied to obtain information regarding body mass (BMI) index, signs and symptoms (i.e., typical chest pain, atypical chest pain, or dyspnea on exertion), risk factors (i.e., diabetes mellitus, hypertension, hypercholesterolemia, or family history), and type of stress test (ceased by exercise or dipyridamole).

According to the obtained information, the mean age of the patients was 54 years regarding the age range from 30 to 85 years. Moreover, 30 patients were over than 50 years old.

According to the results obtained from BMI index, 24 and 16 patients suffered from obesity and overweight, respectively. Table 2 summarizes the results obtained from the study of patient history forms. In the next step, the image contrasts were calculated using equation 4 for the reconstructed images before and after applying the scatter correction.
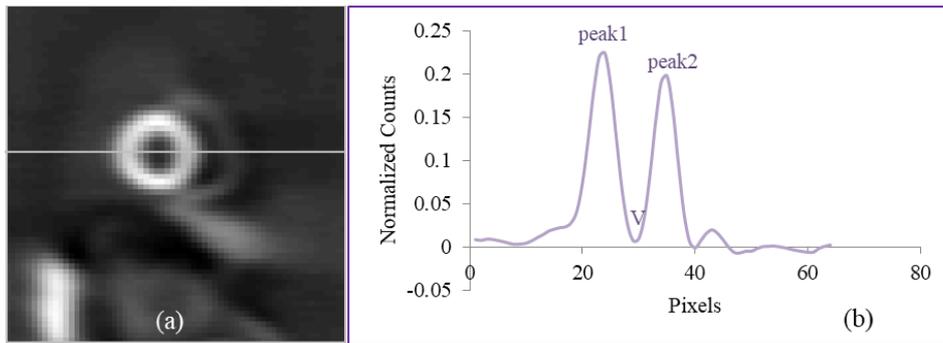

Figure 3. The illustration of (a) a slice of the reconstructed image of 3D-NCAT phantom and (b) two peaks and a valley used in the calculation of the image contrast.

Table 2. The summary of results obtained from the study of patient history forms.

Signs and Symptoms				Risk Factors								Stress Type	
Typical chest pain	Atypical chest pain	dyspnea on exertion	None	Diabetes Mellitus		Hypertension		Hypercholesteromia		Family History		Exercise	Dipyridamole
				Yes	No	Yes	No	Yes	No	Yes	No		
2	24	8	11	7	38	24	21	24	21	11	34	25	20

Results

The simulation study

The results obtained from the simulation showed that 83.4% of the scatter photons detected in the photopeak energy window were the first-order scattered photons. Whereas only 49.4% of the photons detected in the Compton energy window were the first-order scattered photons and the remaining photons (50.5%) were undergone multiple-scattering. Therefore, unlike the assumption used for DEW scatter correction method, it seemed that the spatial distribution of the scatter photons detected in the photopeak window was not similar to that for the photons detected in Compton window (Fig.4). Accordingly, the subtraction of the projections of the Compton window from the projection of the photopeak window based on equation 3, may result in some errors in the scatter corrected image.
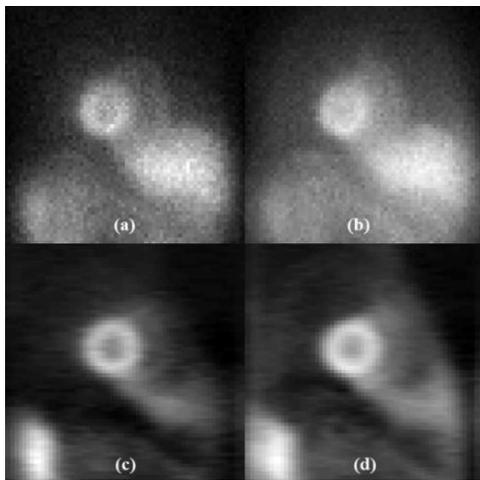

Figure 4. (a) and (b) indicating an arbitrary projection obtained from the scatter counts of photopeak energy window and total counts of Compton energy window, respectively. Moreover, (c) and (d) indicating an arbitrary slice of reconstructed images from these counts for the same energy windows.

The results of linear fitting for a number of arbitrary projections of the 3D-NCAT phantom are given in Table 3. Figure 5 show a sample of this linear fitting. The utilization of the mean values of *a* and *b* obtained from the results of Table 3 is changed equation 3 as follows:

$$S_{pk} = 0.64T_C - 0.16 \tag{5}$$

This equation was employed to correct the projections resulted from the photopeak energy window.
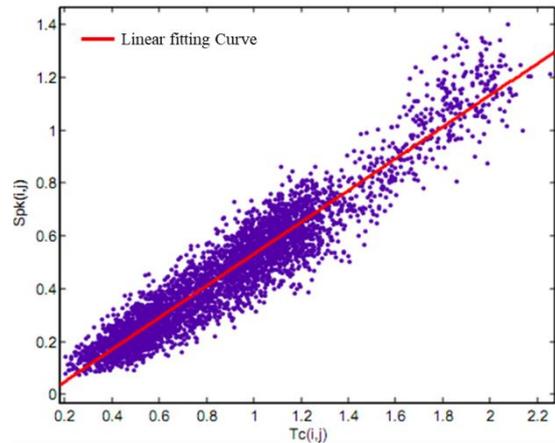

Figure 5. Linear fitting of the pixel counts of an arbitrary same projection obtained from the total counts of Compton energy window (T_C (i,j)) versus the scatter counts of the photopeak energy window (S_{pk}(i,j)).

Table 4 depicts the image contrasts calculated for corrected and uncorrected status by $k = 0.5$ and the linear fitting method before and after reconstruction. As can be seen, the image contrasts are increased after applying the scatter correction using both methods. The level of increase was more using the linear fitting method, compared to the method using constant *k* value slightly.

Table 3. The fitting coefficients of a and b obtained from 17 arbitrary projections of the 3D-NCAT phantom.

Projection Number	a	b
1	0.6081	-0.07652
4	0.6032	-0.07352
8	0.6095	-0.0818
12	0.6159	-0.09034
16	0.6194	-0.09575
20	0.6275	-0.1138
24	0.6471	-0.1439
28	0.6663	-0.1747
32	0.6694	-0.1909
36	0.6705	-0.2055
40	0.6676	-0.2129
44	0.6623	-0.2194
48	0.6549	-0.2191
52	0.6477	-0.214
56	0.6413	-0.2068
60	0.6323	-0.1951
64	0.6286	-0.184
Mean	0.6395	-0.1587

Table 4. The image contrasts calculated for an arbitrary same projection (Fig.6) and a slice of the reconstructed image of the 3D-NCAT phantom (Fig.7) regarding corrected and uncorrected situations by DEW correction method.

Method / Status	NC	DEW	
		$k = 0.5$	Linear Fitting
Projection	0.5365	0.6332 (18.02%)	0.6519 (21.50%)
Reconstructed image	0.8351	0.9295 (10.15%)	0.9553 (12.58%)

Figures 6 and 7 illustrate an arbitrary same projection and a slice of the reconstructed image of the 3D-NCAT phantom regarding the corrected and uncorrected status by DEW method together with the images obtained from the primary photons, respectively. As can be seen, the profile obtained from the corrected images before and after reconstruction is approximately matched with the profile of the primary image, especially for the image corrected by the linear fitting method.

Patient study

It is necessary to notice that because of inaccessibility to the scatter counts of photopeak energy window in a clinical study, it is not possible to use the linear fitting method for the scatter correction. Therefore, the constant value of the k factor ($k=0.5$) was used for the DEW correction method. On the other hand, since the maximum and minimum value of count profile is strongly subjected to image noise, several count profiles were utilized adjacent to each other in reconstructed clinical images.

Afterward, the means of the maximum and minimum values of these profiles were employed to calculate the image contrasts before and after applying the scatter correction. The results obtained from this study are given in Table 5 and 6. Moreover, the results are plotted as a chart in order to make better comparisons (Fig.8).
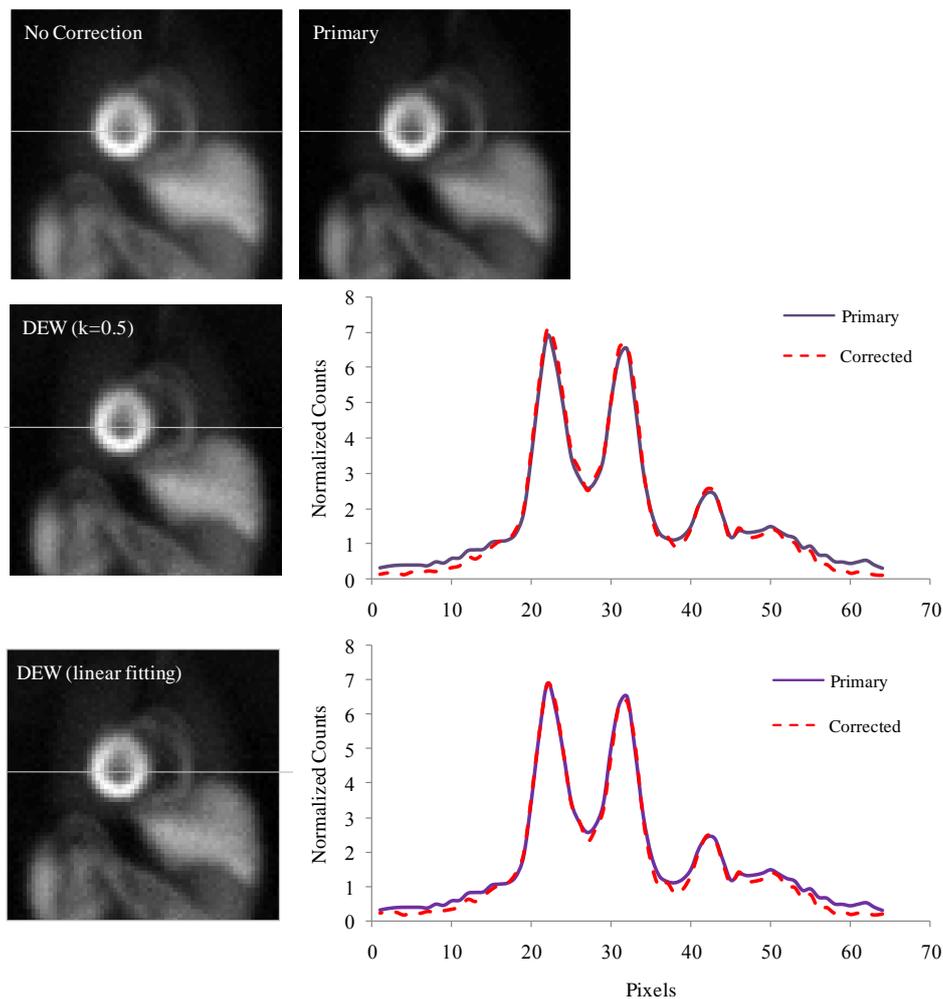

Figure 6. An arbitrary same projection of 3D-NCAT phantom in four situations, uncorrected, primary, and corrected by DEW correction method using $k=0.5$ and linear fitting method
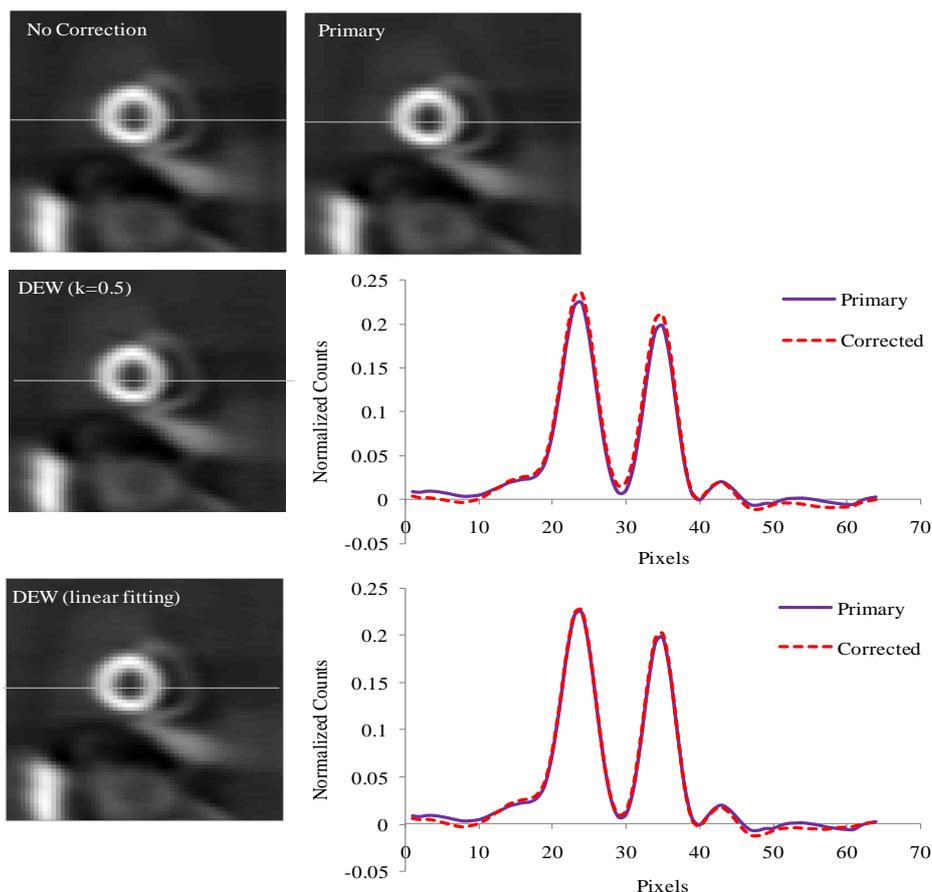
Figure 7. An arbitrary same slice of the reconstructed image of the 3D-NCAT phantom in four situations, uncorrected, primary, and corrected by DEW correction method using $k = 0.5$ and linear fitting method.

Table 5. The image contrasts calculated for uncorrected and corrected images in both rest and stressful situations (27 female patients). The values of standard deviations are in parentheses.

Patient (female)	Rest			Stress		
	NC	SC	Relative increase (%)	NC	SC	Relative increase (%)
1	0.4256	0.4725	11.02	0.5055	0.5612	11.02
2	0.3462	0.4027	16.31	0.322	0.3738	16.10
3	0.6665	0.7529	12.96	0.6912	0.7584	9.727
4	0.5751	0.6655	15.72	0.6736	0.7321	8.689
5	0.6222	0.7188	15.51	0.5634	0.6507	15.49
6	0.7407	0.8446	14.02	0.745	0.8153	9.434
7	0.4728	0.5547	17.34	0.4145	0.4543	9.604
8	0.7473	0.8406	12.48	0.6577	0.7326	11.39
9	0.5931	0.6596	11.21	0.7947	0.8753	10.15
10	0.8656	0.9353	8.049	0.7219	0.7779	7.755
11	0.7107	0.808	13.70	0.676	0.7514	11.16
12	0.697	0.776	11.33	0.5359	0.606	13.07
13	0.5803	0.6856	18.14	0.6125	0.6871	12.18
14	0.4602	0.5109	11.02	0.5296	0.588	11.03
15	0.5922	0.6787	14.62	0.6381	0.7068	10.76
16	0.6252	0.7115	13.80	0.6611	0.7421	12.25
17	0.6388	0.7212	12.89	0.7489	0.8041	7.366
18	0.5505	0.5977	8.564	0.4694	0.4955	5.557
19	0.6204	0.6832	10.12	0.536	0.5936	10.74
20	0.5248	0.59	12.41	0.5749	0.6174	7.386
21	0.5195	0.5991	15.32	0.6806	0.7559	11.06
22	0.6795	0.7622	12.18	0.6823	0.7689	12.69
23	0.4229	0.4974	17.62	0.3171	0.3668	15.65
24	0.7151	0.842	17.74	0.4139	0.4666	12.75
25	0.6429	0.7536	17.22	0.6708	0.7284	8.591
26	0.479	0.5532	15.49	0.4728	0.526	11.26
27	0.5679	0.6323	11.34	0.6639	0.7294	9.863
Mean	0.5956 (0.1169)	0.6759 (0.1284)	13.63 (2.825)	0.5916 (0.1283)	0.6542 (0.1372)	10.84 (2.526)

Table 6. The image contrasts calculated for uncorrected and corrected images in both rest and stressful situations (18 male patients). The values of standard deviations are in parentheses.

| Patient (male)	Rest			Stress		
	NC	SC	Relative increase (%)	NC	SC	Relative increase (%)
1	0.7816	0.8921	14.14	0.3942	0.4304	9.170
2	0.7696	0.8784	14.14	0.7633	0.8369	9.643
3	0.8061	0.8838	9.635	0.844	0.9214	9.169
4	0.7114	0.7726	8.600	0.7628	0.8388	9.966
5	0.6996	0.8016	14.59	0.6469	0.7023	8.553
6	0.6634	0.7599	14.55	0.7557	0.8447	11.78
7	0.6419	0.7077	10.26	0.7054	0.7825	10.93
8	0.8382	0.9236	10.19	0.7899	0.8482	7.391
9	0.5333	0.604	13.26	0.4963	0.5627	13.37
10	0.7035	0.8041	14.30	0.6057	0.667	10.12
11	0.6425	0.7124	10.89	0.7068	0.7692	8.828
12	0.6821	0.7626	11.80	0.7342	0.8087	10.15
13	0.8145	0.9125	12.04	0.5186	0.5709	10.08
14	0.8041	0.9097	13.14	0.8743	0.9566	9.407
15	0.8369	0.9588	14.56	0.6518	0.7274	11.59
16	0.5355	0.5853	9.301	0.5143	0.5998	16.63
17	0.7081	0.7827	10.530	0.6243	0.7037	12.71
18	0.6578	0.7298	10.94	0.7025	0.7768	10.58
Mean	0.7082 (0.0879)	0.7937 (0.1014)	12.03 (2.052)	0.6717 (0.1282)	0.7416 (0.1359)	10.56 (2.112)
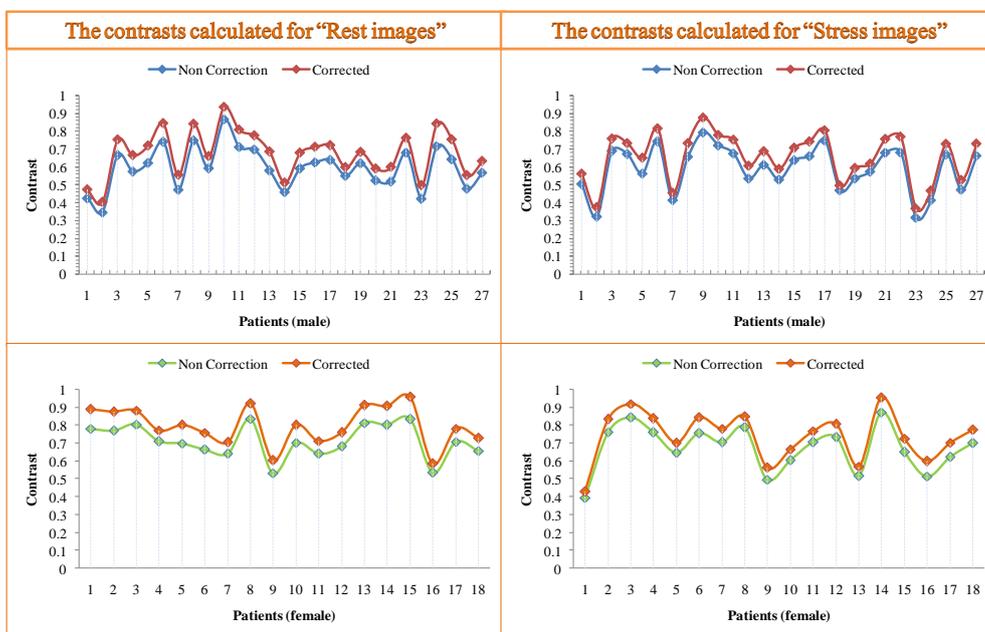
Figure 8. The chart plotted from the data in Table 5 and 6. The image contrasts increasing after applying the scatter correction.

The results of the clinical study indicated that the scatter correction improved the contrasts of the images for males and females in both rest and stressful situations. Moreover, the mean of the relative increase in the rest situation is more than that in the stressful situation. According to the results obtained from the tables, the image contrasts calculated for the female patients are lower than those for the male ones due to the presence of the breast tissue. Figure 9 illustrates a projection and two slices of the reconstructed image before and after applying the scatter correction.
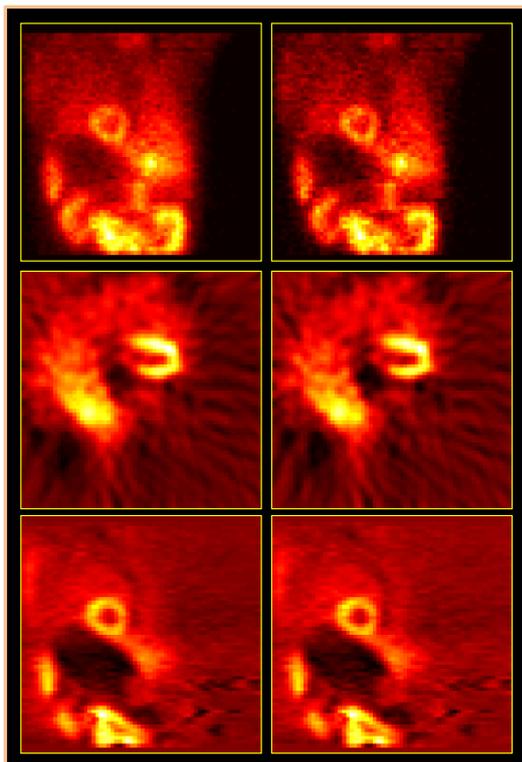
Figure 9. A sample of the images obtained before (left column) and after (right column) applying the scatter correction. The first, second, and third rows are projections before the reconstruction, a transverse slice, and a coronal slice of the reconstructed image for a male patient, respectively.

Discussion

The detection of photons undergoing Compton scattering into the main energy window of imaging (photopeak window) leads to the degradation of image contrast, and therefore reduces the accuracy of image quality and quantity (19). That is the reason why researchers pay much attention to find a way to reduce the scattering effects in nuclear medicine imaging (20). Several studies performed in this field have been used phantoms to evaluate the scatter correction, such as our previous study (14) that was conducted on six scatter correction methods based on setting the energy windows in Tc-99m energy spectrum. These methods was evaluated using a cylindrical phantom including six spheres with different diameters. The image contrasts and signal-to-noise ratios calculated for six cold-spheres revealed that the DEW and triple-energy window (TEW) correction methods were two suitable methods for the scatter correction of images.

Furthermore, in another study (15), a new approximation was proposed for the scatter correction with a slight modification in the TEW method. This modification was made by setting an additional narrow energy window at 133 keV leading to more increase in the image contrasts, compared to TEW scatter correction method. There is a dearth of research regarding the investigation of scatter correction on patients. Changizi et al. (21) investigated the effect of TEW method on a group of patients, including 43 males

and 37 females. The results of this study showed that the sensitivity and specificity increased from 86% to 94% and from 61% to 84%, respectively. In another study performed by Rafati et al. (22), three scatter correction methods were evaluated based on setting energy windows in Tc-99m energy spectrum using simulation and clinical data. The results of their study showed that the image contrasts improved after the scatter correction by all three methods. Moreover, Blokland et al. (23) investigated the effect of TEW method in Tl-201 myocardium perfusion imaging. The investigation performed on the images obtained from 30 patients showed that the image contrast improved significantly by applying the scatter correction. However, the signal-to-noise ratio decreased in this study.

The aim of this study was to evaluate the efficiency of DEW method proposed by Jaszczak et al. (3) for scatter correction of images obtained from SPECT imaging using simulation and patient data. In this correction method that is simply applicable in the nuclear medicine imaging systems, it is assumed that the scatter counts detected into the photopeak energy window (126-154 keV) can be estimated by multiplication of a k factor in the total counts detected into the Compton energy window (92-154 keV).

In this simulation study, 3D-NCAT phantom and two approaches were utilized to apply the scatter correction. These two approaches include the use of a constant value for k factor ($k = 0.5$ proposed by Jaszczak et al.) and the linear fitting method of the data.

According to the results obtained from Table 4, the image contrast increased after applying the scatter correction by both approaches. In addition, the relative increase in the second approach (12.58%) was more than that in the first approach (10.15%). In the next stage, the images obtained from 45 patients, including 27 males and 18 females, were evaluated in both rest and stressful situations. The results obtained from this stage (Tables 5 and 6) showed that the image contrast improved regarding all patients after applying the scatter correction. The mean values of increase considering the female patients were from 0.5956 to 0.6759 and 0.5916 to 0.6542 for rest and stressful situations, respectively. However, mean values of increase regarding male patients were from 0.7082 to 0.7937 and 0.6717 to 0.7416 for rest and stressful situations, respectively. The results of this study revealed that regarding both groups of patients, the rest situation obtained higher levels of the relative increase in image contrast, compared to the stressful situation. This difference between female and male patients was 2.79% and 1.74%, respectively.

Conclusion

This study investigated the DEW scatter correction method using simulation and patient data. According to the results obtained from the simulation study which used two approaches, the DEW scatter correction method led to an increase in the contrast of the images. Moreover, the results of the clinical study indicated that the image contrasts improved after performing the

scatter correction in both rest and stressful situations regarding female and male patients. Therefore, according to the findings of the simulation and patient studies, it can be concluded that the use of the DEW scatter correction method causes an increase in the image contrast, and therefore improves the diagnostic accuracy.

Acknowledgment

References

1. DePuey EG, Garcia EV, Berman DS. Cardiac SPECT Imaging. Lippincott Williams & Wilkins; 2001.
2. Nishimura S, Mahmarian JJ, Boyce TM, Verani MS. Quantitative thallium-201 single-photon emission computed tomography during maximal pharmacologic coronary vasodilation with adenosine for assessing coronary artery disease. Journal of the American College of Cardiology. 1991 Sep 1;18(3):736-45.
3. Jaszczak RJ, Greer KL, Floyd JC, Harris CC, Coleman RE. Improved SPECT quantification using compensation for scattered photons. Journal of nuclear medicine: official publication, Society of Nuclear Medicine. 1984 Aug;25(8):893-900.
4. Axelsson B, Msaki P, Israelsson A. Subtraction of Compton-scattered photons in single-photon emission computerized tomography. Journal of nuclear medicine: official publication, Society of Nuclear Medicine. 1984 Apr;25(4):490-4.
5. Floyd JC, Jaszczak RJ, Greer KL, Coleman RE. Deconvolution of Compton scatter in SPECT. Journal of nuclear medicine: official publication, Society of Nuclear Medicine. 1985 Apr;26(4):403-8.
6. Jaszczak RJ, Floyd CE, Coleman RE. Scatter Competition Techniques for SPECT. IEEE Trans. Nucl. Sci. 1985; 32: 786-93.
7. Gilardi MC, Bettinardi V, Todd-Pokropek A, Milanesi L, Fazio F. Assessment and comparison of three scatter correction techniques in single photon emission computed tomography. Journal of nuclear medicine. 1988 Dec 1;29(12):1971-9.
8. Ogawa K, Harata Y, Ichihara T, Kubo A, Hashimoto S. A practical method for position-dependent Compton-scatter correction in single photon emission CT. IEEE transactions on medical imaging. 1991 Sep;10(3):408-12.
9. Logan KW, McFarland WD. Single photon scatter compensation by photopeak energy distribution analysis. IEEE transactions on medical imaging. 1992 Jun;11(2):161-4.
10. King MA, Hademenos GJ, Glick SJ. A dual-photopeak window method for scatter correction. J Nucl Med. 1992 Apr 1;33(4):605-12.
11. Pretorius PH, van Rensburg AJ, van Aswegen A, Lötter MG, Serfontein DE, Herbst CP. The channel ratio method of scatter correction for radionuclide image quantitation. Journal of Nuclear Medicine. 1993 Feb 1;34(2):330-5.
12. Ljungberg M, King MA, Hademenos GJ, Strand SE. Comparison of four scatter correction methods using Monte Carlo simulated source distributions. Journal of Nuclear Medicine. 1994 Jan 1;35(1):143-51.
13. Buvat I, Rodriguez-Villafuerte M, Todd-Pokropek A, Benali H, Di Paola R. Comparative assessment of nine scatter correction methods based on spectral analysis using Monte Carlo simulations. Journal of Nuclear Medicine. 1995 Aug 1;36(8):1476-88.
14. Asl MN, Sadremomtaz A, Bitarafan-Rajabi A. Evaluation of six scatter correction methods based on spectral analysis in 99mTc SPECT imaging using SIMIND Monte Carlo simulation. Journal of Medical Physics/Association of Medical Physicists of India. 2013 Oct;38(4):189.
15. Noori-Asl M, Sadremomtaz A, Bitarafan-Rajabi A. Evaluation of three scatter correction methods based on estimation of photopeak scatter spectrum in SPECT imaging: A simulation study. Physica Medica. 2014 Dec 1;30(8):947-53.
16. Segars WP, Lalush DS, Tsui BM. Modeling respiratory mechanics in the MCAT and spline-based MCAT phantoms. IEEE Transactions on Nuclear Science. 2001 Feb;48(1):89-97.
17. Ljungberg M, Strand SE. A Monte Carlo program simulating scintillation camera characteristics. Computer Methods and Programs in Biomedicine. 1989; 29:257-72.
18. Segars WP, Tsui BM. Study of the efficacy of respiratory gating in myocardial SPECT using the new 4-D NCAT phantom. IEEE Transactions on Nuclear Science. 2002 Dec 10;49(3):675-9.
19. Pirayesh Islamian J, Bahreyni Toossi MT, Momennezhad M, Zakavi SR, Sadeghi R. Monte Carlo Study of the Effect of Backscatter Material Thickness on 99mTc Source Response in Single Photon Emission Computed Tomography. Iranian Journal of Medical Physics. 2013 Mar 1;10(1):69-77.
20. Hutton BF, Buvat I, Beekman FJ. Review and current status of SPECT scatter correction. Physics in Medicine & Biology. 2011 Jun 23;56(14): 85-112.
21. Changizi V, Takavar A, Babakhani A, Sohrabi M. Scatter correction for heart SPECT images using TEW method. Journal of applied clinical medical physics. 2008 Jun;9(3):136-40.
22. Rafati M, Rouhani H, Bitarafan-Rajabi A, Noori-Asl M, Farhood B, Ahangari HT. Assessment of the scatter correction procedures in single photon emission computed tomography imaging using simulation and clinical study. Journal of Cancer Research and Therapeutics. 2017;13(6):936-42.
23. Tot Nederveen WH, Van Eck-Smit BL, Pauwels EK. Scatter correction on its own increases image contrast in TI-201 myocardium perfusion scintigraphy, but does it also improve diagnostic accuracy?. Annals of nuclear medicine. 2003 Dec 1;17(8):725-31.